Molecular BioSystems

PAPER

View Article Online
View Journal

Cite this: DOI: 10.1039/c7mb00185a

Aggregation behavior of novel heptamethine cyanine dyes upon their binding to native and fibrillar lysozyme†

Kateryna Vus,*[a] Ulyana Tarabara,[a] Atanas Kurutos,[b] Olga Ryzhova,[a] Galyna Gorbenko,[a] Valeriya Trusova,[a] Nikolai Gadjev[b] and Todor Deligeorgiev[b]

Received 26th March 2017,
Accepted 28th March 2017

DOI: 10.1039/c7mb00185a

rsc.li/molecular-biosystems

Two newly synthesized symmetrical heptamethine cyanine dyes, AK7-5 and AK7-6, absorbing in the region of low autofluorescence of biological samples, have been tested for their ability to detect proteins aggregated into amyloid fibrils. In aqueous solution these probes possess three absorption bands corresponding to the monomer, dimer and H-aggregate species. The association of the dye with fibrillar lysozyme was followed by the enhancement of the monomer band and the reduction of the H-band. The absorption spectra measured at various fibril concentrations were analyzed in terms of the model allowing for the shift of equilibria between various dye species due to the binding of monomers and dimers of AK7-5 and AK7-6 to amyloid fibrils. The association constants and stoichiometries of the dye–fibril complexation have been evaluated. In contrast to fibrillar lysozyme, the native protein brought about strong J-aggregate formation accompanied by a marked drop in the absorbance of the dye monomer species. Quantum chemical calculations and simple docking studies showed that AK7-5 and AK7-6 monomers can bind to the grooves, running parallel to the fibril axis. Due to their ability to distinguish between the native and fibrillar protein states, the novel cyanines are recommended as complementary to existing amyloid markers.

Introduction

Near-infrared (NIR) cyanine dyes have found numerical applications in a variety of research areas including bioanalytics, optoelectronics, photoelectrochemistry, laser technologies, *etc.*[1–3] Likewise, these probes have been employed as non-covalent labels for the detection of proteins,[4] nucleic acids,[5] lipids,[6] and strong oxidizing agents (*viz.*, peroxynitrite ($ONOO^-$), hypochlorous acid (HOCl), *etc.*)[7,8] due to their advantages, such as, particularly, high extinction coefficients[9,10] and long-wavelength absorption and fluorescence maxima.[11] The latter prevents the overlapping of the dye spectra with those of the investigated samples, ensuring deep penetration of the absorbed light into the tissues. The second interesting property of cyanines is their ability to form self-associated structures stabilized by van der Waals, H-bonding, electrostatic, steric, hydrophobic and stacking intermolecular interactions.[12,13] Upon self-association these dyes form two types of aggregates, H and J, whose absorption spectra are shifted to short- and long-wavelength regions relative to the monomer band, respectively.[14] The origin of this shift was explained by the exciton theory, predicting how the aggregate type depends on the transition moment arrangement of the point dipoles of individual dye molecules.[15] Due to the interaction between the transition dipoles, the exciton state of the aggregate splits into two levels.[16] The parameter that describes the disposition of the dye molecule is the slippage angle α, which is defined as the angle between the direction of any one of the parallel molecules and the line of the center of the aggregate. In particular, when $\alpha = 90^\circ$ the molecules are in parallel orientation and form "plane-to-plane" stacks ("card-pack" arrangement). In this case only the upper state transition is allowed, corresponding to the hypsochromic shift characteristics of the H-aggregates. Meanwhile, when $\alpha = 0^\circ$ a linear molecular orientation is observed, namely "end-to-end" stacking ("brickwork" arrangement).[17] In a general case, the slippage angles fall in the range of $\{90^\circ–32^\circ\}$ for the H-aggregates and $\{32^\circ–0^\circ\}$ for the J-aggregates.[10]

Importantly, changes in the environmental conditions may shift the monomer–aggregate equilibria, resulting in mutual conversions between the dye species. Specifically, aggregate formation is a function of temperature, solvent polarity, pH and ionic strength.[17] For example, cyanines undergo disaggregation

[a] *Department of Nuclear and Medical Physics, V.N. Karazin Kharkiv National University, 4 Svobody Sq., Kharkiv, 61022, Ukraine. E-mail: kateryna.vus@yahoo.com*

[b] *Faculty of Chemistry and Pharmacy, Sofia University, "St. Kliment Ohridski", 1, blv. J. Bourchier, Sofia, 1164, Bulgaria*

† Electronic supplementary information (ESI) available. See DOI: 10.1039/c7mb00185a

when being transferred from an aqueous phase to nonpolar solvents,[18] from neutral to acidic buffer or upon heating.[19,20] In turn, salt-induced J-aggregate formation was observed for thiacarbocyanine dyes, accompanied by the disruption of the H-aggregates.[21] To reproduce the cyanine dye spectral behavior in buffer upon increasing the dye concentration, the monomer–H-aggregate and/or monomer–J-aggregate equilibria must be considered.[20,22] Furthermore, to describe quantitatively the dye binding to biological molecules, one should analyze the monomer–aggregate and the dye–biomolecule binding equilibria.[22,23] Such an approach has been employed, for instance, while analyzing the interaction between the novel heptamethine cyanine dye and human serum albumin.[11]

Remarkably, cyanine dyes have been successfully employed for the detection of a specific type of protein aggregate – amyloid fibrils, whose formation is involved in the pathogenesis of Alzheimer's disease, systemic amyloidosis, *etc.*[24] These aggregates are typically tens of nanometers in width and several micrometers in length, sharing a core cross-β-sheet structure, in which β-strands run perpendicularly to the long axis of the fibril, while β-sheets propagate in its direction.[25] To exemplify, pinocyanol dye appeared to be more sensitive to Aβ-fibrils than Congo Red,[26] trimethine cyanines T-49 and SH-516 exhibited substantial fluorescence increases in the presence of fibrillar beta-lactoglobulin and α-synuclein,[27] and novel thiacarbocyanines,[28] trimethine cyanine dye 7519[29] and carbazole-based cyanines[30] were used as anti-amyloid drugs. Notably, the ability of the dyes to inhibit amyloid fibril formation is connected with their tendency to form aggregates in solution due to strong stacking interactions with aromatic amino acids, as was shown for phthalocyanines, Congo Red, *etc.*[31,32] The advantages of cyanine dyes over Thioflavin T include not only their absorption in the NIR region but also more pronounced fluorescence (absorbance) changes in the presence of fibrils and high reproducibility of the results.[33]

However, cyanine dyes for bioimaging applications suffer from several drawbacks: (i) low photostability in aqueous solutions due to flexibility of the polymethine chain,[34,35] (ii) poor water solubility,[36] (iii) small Stokes shifts,[37] and (iv) high tendency to form aggregates in polar and nonpolar solvents that complicates spectral data analysis. Specifically, symmetrical carbocyanine dyes possess a high aggregation potential in buffer due to strong dispersion interactions between the planar dye species[38] and H-bonds formed between the dye and water molecules.[39] Furthermore, disadvantages of using clinically established NIR dyes, *viz.* indocyanine green (ICG), as contrast agents for *in vivo* fluorescence imaging, include: (i) low quantum yield in buffer,[40] (ii) non-covalent binding to plasma proteins,[41] (iii) cytotoxicity, and (iv) low thermal stability.[39] Notably, the twisted intramolecular charge transfer (TICT) state of cyanine dyes is stabilized in water, although the rate of transfer from the locally excited to the TICT state is lowered in a viscous environment.[42] Aggregation,[43] photoisomerization,[44] torsional rotation (followed by TICT formation) and H-bonding between the dye and protic solvent[45] reduce the dye quantum yield and fluorescence lifetime in the free state as compared to the lipid-, DNA- and protein-associated states, making them weak contrast agents but promising noncovalent fluorescent markers for biomolecules. Interestingly, the mechanisms of fluorescence quenching of cyanines are similar to those reported for, *e.g.*, Oxazine 750,[46] Pchlide,[47] fluorenone,[48] *etc.* In view of the above, the development of novel cyanine dyes possessing higher stability and water solubility along with low cytotoxicity is important for further progress in medical diagnostics.[36] For instance, heptamethine cyanine dyes containing four sulfo groups had greater water solubility and photostability compared to those containing one sulfo group.[49] In turn, rigidifying the heptamethine chain by the incorporation of the bulky moieties, *viz.* benz[*e*]indolium moiety, piperidine, diphenylamine, chlorocyclohexenyl and carbocyclic rings, *etc.*, results in the attenuation of aggregation, photoisomerization and TICT formation of the cyanine dyes in buffer.[50,51]

Recently, we have reported the marked spectral changes of the novel symmetrical heptamethine cyanine dyes AK7-5 and AK7-6 in the presence of DNA, bovine serum albumin (BSA) and phospholipids, suggesting their applicability to the studies of biological molecules.[52] These probes possess a rigid chlorocyclohexenyl ring in the polymethine chain, providing high photostability and quantum yield in buffer.[37] Furthermore, cyanines with a pentyl or longer polymethine chain had stronger binding affinity for DNA and BSA than the dyes with a shorter link-chain.[52] In view of this, the present study was aimed at the quantitative characterization of the interactions between AK7-5, AK7-6 and native/fibrillar lysozyme, taking into account the dye monomer–aggregate equilibria in buffer. The parameters of dye–protein binding have been estimated and putative fibril binding sites have been suggested, thus providing a basis for assessing the potential of the novel dyes as noncovalent markers for amyloid fibrils.

Materials and methods

Experimental

Hen egg white lysozyme and Tris–HCl were obtained from Sigma (USA). Cyanine probes AK7-5 and AK7-6 (Fig. 1) were synthesized in the University of Sofia, Bulgaria, as described previously.[53] Stock solutions of AK7-5 and AK7-6 were prepared by dissolving the dyes in DMSO, then diluted in 10 mM Tris–HCl buffer (pH 7.4) and used for spectroscopic measurements. The concentration of the dyes was determined spectrophotometrically, using the extinction coefficients ε_{808}^{DMSO} = 0.197 μM^{-1} cm^{-1} and ε_{814}^{DMSO} = 0.209 μM^{-1} cm^{-1} for AK7-5 and AK7-6, respectively. Lysozyme amyloid fibrils were grown by incubation of the protein solution (10 mg ml^{-1}) in 10 mM glycine buffer (pH 2) at 60 °C for 14 days.[53] The working solutions of native and fibrillar lysozyme were prepared in 10 mM Tris–HCl buffer (pH 7.4). To estimate the equilibria constants for H-dimer and H-aggregate formation, the absorption spectra were recorded upon increasing the dye concentration using a CM-2203 spectrometer (SOLAR, Belarus). To qualitatively analyze the dye–lysozyme binding, AK7-5 and AK7-6 solutions were titrated with the protein.

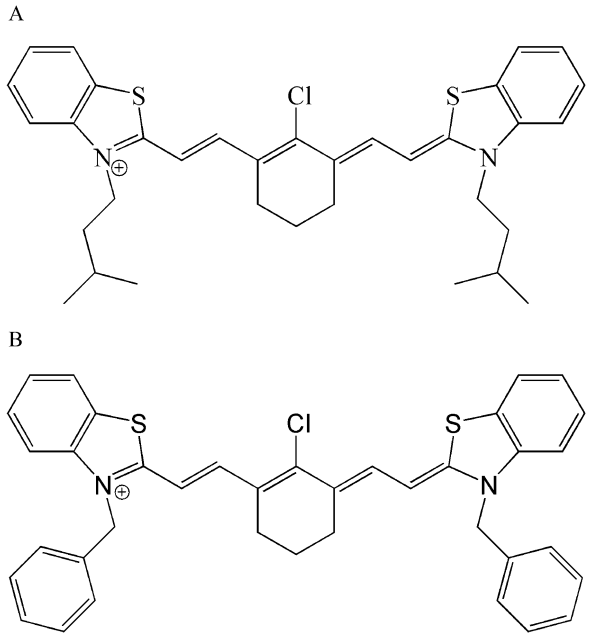

Fig. 1 Structures of the AK7-5 and AK7-6 dyes.

Quantum chemical calculations

The energy of the highest occupied (E_{HOMO}) and the lowest unoccupied (E_{LUMO}) molecular orbitals, the solvent-accessible area (CA), the cosmo volume (molecular volume) (CV), and the molecular length (L), width (W) and height (H) were calculated by the semiempirical PM6 method using MOPAC 2012.[54] The dipole moment of the ground state (μ_g) was determined using Win-Gamess and the 6-31G(d,p) basis set, density functional theory (DFT) and the B3LYP functional.[55] The semiempirical AM1 method with added polarization (1) and diffuse (1) functions on heavy atoms, and a polarization function on hydrogen atoms were employed for the ground-state geometry optimization of the heptamethine cyanine dyes. The HOMO and LUMO shapes (Fig. S1, ESI†) were calculated with the 6-31G(d,p) basis set, using time-dependent density functional theory (TDDFT) and the ground-state optimized geometries.[56] The AlogPS method from the Virtual Computational Chemistry Laboratory (http://www.vcclab.org) was used for the calculation of lipophilicity of the examined compounds ($C\,\mathrm{Log}\,P$). The obtained results are provided in Table S1, ESI.† Notably, the dihedral angles of the dye skeleton were close to 0°–22°, indicating the planarity of the novel cyanines.

Docking studies

The crystal structure of hen egg white lysozyme (PDB ID: 3A8Z) was taken from the Protein Data Bank. Lysozyme fibril was built from the K-peptide, GILQINSRW (residues 54–62 of the wild-type protein), using the CreateFibril tool as described previously.[57,58] The geometry of AK7-5 and AK7-6 monomers was optimized as described above. The docking models of the dye dimers and their complexes between the dye monomer (dimer) and native or fibrillar lysozyme were obtained using the PatchDock algorithm, which is a user-friendly tool for the calculation of the optimal structures of the protein–drug and protein–protein complexes.[59] The online available program searches the transformations of the two interacting molecules (assuming the proteins to be rigid bodies), revealing the maximized surface shape complementarity and the minimized number of steric clashes. The top 10 obtained conformations were then refined by the FireDock algorithm, which calculates the optimal rearrangement of the side chains in the protein–ligand complex by the Monte Carlo minimization of the binding score function (comprising the following important contributants – energy of ligand–protein van der Waals interactions and desolvation free energy).[60] The docked complexes were visualized by the Visual Molecular Dynamics (VMD) software.

Results and discussion

Estimation of the equilibrium constants for AK7-5 and AK7-6 aggregation in buffer

As shown in Fig. 2A, the AK7-5 monomer has an absorption maximum at 808 nm in DMSO, while the dye spectrum in aqueous solution can be decomposed into at least 4 different components, corresponding, presumably, to the dye monomers (M, $\lambda_{max} \sim 808$ nm), H-dimers (D, $\lambda_{max} \sim 700$ nm) and higher order H-aggregates (H1, $\lambda_{max} \sim 595$ and H2, $\lambda_{max} \sim 640$ nm). The absorption maximum of the AK7-6 monomer in DMSO is 815 nm, while those of H1, H2, D and M are about 595 nm, 630 nm, 695 and 815 nm, respectively (Fig. 2B). Bis-heptamethine cyanine dyes have been reported to form predominantly H-dimers

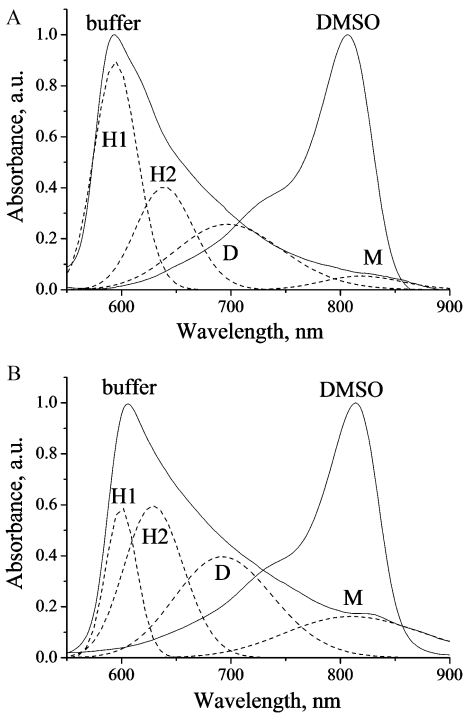

Fig. 2 Normalized absorption spectra of AK7-5 (A) and AK7-6 (B) in DMSO and buffer. The deconvoluted spectral bands correspond to the H-aggregate (H1, H2), H-dimer (D) and monomer (M) species. The AK7-5 and AK7-6 concentrations were 12.2 and 13.5 μM, respectively.

in aqueous solution.[16] The formation of H-aggregates in buffer starts at lower probe concentrations[61] as compared to those (*ca.* 10^{-5} to 10^{-3} M^{-1}) required for dye J-aggregation.[62] Notably, some amount of AK7-5 and AK7-6 J-aggregates could appear in buffer, as judged from the broadening of the monomer absorption bands.[13,63] Indeed, the incorporation of positively charged or bulky groups to the dye molecule resulted in the enhancement of J-aggregation.[64,65] Furthermore, the exciton theory predicts that the larger the aggregate size, the larger the hypsochromic/bathochromic shifts of the H-/J-bands relative to the monomer band.[15,20]

Numerous approaches have been employed to qualitatively describe cyanine aggregation in aqueous solutions. To exemplify, Taticolov and coworkers have estimated the aggregation constant and the number of anionic cyanine dyes from the double-logarithmic plots of the J-aggregate absorbance *versus* the monomer absorbance.[23] Analysis of the average value of the extinction coefficient of naphthalocyanines observed at a certain wavelength yielded $n \sim 1.5$–2.0 and $K_{agg} \sim 4.5 \times 10^{-3}$–$3.1 \times 10^{-2}$ μM^{-1}.[66] Assuming the simplest case, *i.e.* the monomer–dimer equilibrium, the dimerization constants were estimated by a number of graphical methods, revealing values of *ca.* $(3.8–8.5) \times 10^{-3}$ μM^{-1} for benzindocarbocyanine dyes;[67] *ca.* 2.6×10^{-3} μM^{-1} for mononuclear cobalt phthalocyanines;[63] *ca.* $(7.4–110) \times 10^{-3}$ μM^{-1} and $n \sim 1.2$–1.7 for thiacyanines;[64] and *ca.* 7.4–9.3 for the tetrasulfonated phthalocyanines,[66] *etc.* In a general case, for the monomer–*n*-aggregate equilibria, the numerical solution of the equation, which describes the balance between the total probe concentration and the amounts of the monomer, dimer,…, *n*-aggregate species, could be found, revealing the concentration of the monomer species in buffer and the averaged aggregation constant $K_n^{tot} = K_1 \cdot K_2 \ldots K_n$, where K_1, K_2, …, K_n are the constants of the dye dimerization, trimerization,…, and *n*-merization, respectively. This approach was employed, for instance, by Schutte and coworkers for octalosubstituted phthalocyanine, in which the values of $K_1 = 1.5$ μM^{-1} and $K_1 \cdot K_2 = 0.08$ μM^{-2} were obtained.[67]

Therefore, in order to characterize the processes occurring in the dye–protein system, we first directed our efforts towards the estimation of the equilibrium constants for the H-dimer (K_d) and H-aggregate (K_h) formation, and the averaged dye aggregation number (n) in buffer, assuming the existence of dye monomer–H-dimer and dye–H-aggregate equilibria:[22,23]

$$nC_m \rightleftarrows C_h, \quad K_h = \frac{C_h}{C_m^n} \tag{1}$$

$$2C_m \rightleftarrows C_d, \quad K_d = \frac{C_d}{C_m^2} \tag{2}$$

$$C_m + 2K_d C_m^2 + nK_h C_m^n = C_0, \tag{3}$$

where C_m, C_d, C_h, and C_0 are the concentrations of the dye monomers, H-dimers, and H-aggregates, and the total dye concentration, respectively. The numerical solution of eqn (3) performed by simultaneous analysis of the absorption spectra measured at varying C_0 yielded rather realistic values of the aggregation number and equilibrium constants, *viz.* {K_h = 85 μM^{-1}, K_d = 7 μM^{-1}, n = 4} and {K_h = 120 μM^{-1}, K_d = 5 μM^{-1}, n = 4} for AK7-5 and AK7-6, respectively, the values being similar to those reported for cyanines elsewhere.[23,65] The recovered parameters were further used to calculate the dye monomer, H-dimer and H-aggregate concentrations, plotted as a function of the total dye concentration in Fig. S2A and S3A (ESI†), respectively. It appeared that the amounts of dye monomers in the H-aggregate and free monomer species were the highest and the lowest, respectively, within the examined C_0 range. The observed trend is in good agreement with the measured band intensities of the dye species in buffer (Fig. 2). Furthermore, the discrepancy between the measured and calculated absorbances of AK7-5/AK7-6 monomers, H-dimers and H-aggregates (the values were taken from the deconvoluted dye spectra) was found to be the lowest for $\varepsilon_d = 0.1/0.197$ μM^{-1} cm^{-1} and $\varepsilon_h = 0.05/0.1$ μM^{-1} cm^{-1}, where ε_d and ε_h are the extinction coefficients of the dye monomers in the H-dimers and H-aggregates, respectively. Fig. S2B–D and S3B–D (ESI†) represent the measured and calculated absorbances at the wavelengths corresponding to the monomer, dimer and H-aggregate dye species, over the overall dye concentration range. Our results agree with the fact that extinction coefficients of the dye monomers in the H-dimer and higher order H-aggregates are lower than that of monomer species.[13,16] The value of K_h for AK7-6 exceeds that of AK7-5 by ~30%, presumably due to stronger dispersion forces between the two AK7-6 molecules.[39] Indeed, the structure of AK7-6 dimers should be more planar than that of AK7-5 due to the stronger stacking interactions between the monomer species. Furthermore, the ground-state dipole moment of AK7-6 is 2 times higher than the corresponding value for AK7-5 (Table S1, ESI†), suggesting a greater Gibbs free energy change upon dye–dye binding.[68] The recovered parameters, characterizing the dye monomer–aggregate equilibria in buffer, were further employed to describe the spectral behavior of the examined cyanines in the presence of native and fibrillar lysozyme.

Cyanine dye response to native lysozyme

Upon addition of native lysozyme to AK7-5 and AK7-6 in the aqueous phase, the following effects have been observed: (i) a marked decrease in the absorbance of H-aggregates, augmenting with increasing protein concentration (Fig. S4A and B, ESI†); (ii) a rise in the relative contribution of the H2 band to the overall spectrum (Fig. 2 and Fig. S4C, D, ESI†); and (iii) a slight absorbance increase at ~840 nm (55% and 26% at the maximum protein concentration, respectively) (Fig. S4A and B, ESI†). While considering the dye–protein interactions, it is important to find out what kinds of dye species participate in this process.

Hypothesis 1. First, we supposed that the binding of the dye monomers to native lysozyme results in the shift of aggregation equilibria, *i.e.* disruption of the dye H-aggregates (Fig. S4, ESI†). Indeed, both the dye–protein complexes and the dye aggregates are stabilized by the same types of intermolecular interactions (van der Waals, H-bonding, electrostatic and hydrophobic),[12,13] and dye disaggregation could occur as a result of the competition between dye–protein and dye–dye binding.[11,62] The disruption

of cyanine H-aggregates has been observed in the presence of peptides and human serum albumin, indicating that dye–protein complexation is more energetically favourable than aggregate formation.[2,16] Notably, the monomer species of phthalocyanine dyes have been found to interact with native insulin, with the low-order self-associated dyes playing a minor role in this process.[19] To test the validity of this hypothesis, an additional relationship should be added to the above set of equations {(1)–(3)}:

$$C_m + P \rightleftarrows C_{mp}, \quad K_b = \frac{C_{mp}}{C_m(mP - C_{mp})} \qquad (4)$$

where C_{mp}, P, K_b, and m are the concentration of the protein-bound monomers, the lysozyme concentration, the association constant and the stoichiometry of dye–protein binding, respectively. Notably, the C_{mp} addendum was included into eqn (3). By solving the equation set {(3) and (4)}, we made an attempt to reproduce the spectral behavior of the examined dyes in the presence of lysozyme through looking for the appropriate set of parameters {K_b, m}. However, we failed to obtain reasonable values of the above parameters capable of providing good agreement between the experiment and theory. For instance, for {K_b = 0.02 μM^{-1}, m = 1} at the maximum protein concentration 35.3 μM, the discrepancy between the experimental and calculated values of A_{640} for AK7-5 was about 18%, while the calculated values of A_{700} and A_{840} were greater than the experimental ones by factors of ~2.5 and ~2, respectively. Similarly, for {K_b = 0.04 μM^{-1}, m = 1} at the maximum protein concentration of 35.7 μM, the discrepancy between the experimental and calculated A_{600} for AK7-6 was about 33%, while the calculated values of A_{700} and A_{840} were lower and greater than the experimental ones by factors of ~2 and ~1.5, respectively. Fig. S5 (ESI†) represents the measured and calculated absorbances at 640/600, 700 and 820 nm over the overall protein concentration range. The obtained discrepancies between the experiment and theory imply that the assumption about dye H-aggregate disruption as a result of dye monomer binding to the native protein cannot *per se* explain the observed spectral effects. Notably, the extinction coefficients were taken as 0.05/0.1 (H-aggregates) and 0.1/0.197 (H-dimers) μM^{-1} cm^{-1} for AK7-5 and AK7-6, respectively, while ε_{840} was assumed to be similar for free and bound monomer species (ε_{840} = 0.197 μM^{-1} cm^{-1}). Indeed, the absorptivity values of the protein-bound dye monomers appeared to be close to those of the free dye species, as was shown, *e.g.*, for Thioflavin T and Congo Red.[69,70]

Hypothesis 1a. In order to eliminate the above discrepancies between the experiment and theory, it was suggested that both the dye monomers and H-dimers could bind to native lysozyme, leading to the shift of aggregation equilibria. This requires the inclusion of an additional equation into the above set {(1)–(4)}:

$$C_d + P \rightleftarrows C_{dp}, \quad K_{bd} = \frac{C_{dp}}{K_d C_m{}^2(m_d P - C_{dp})}, \qquad (5)$$

where C_{dp} is the concentration of the lysozyme-bound H-dimers, and K_{bd} and m_d are the association constant and stoichiometry for H-dimer–protein binding, respectively. Notably, the C_{mp} and $2{\cdot}C_{dp}$ addenda were included into eqn (3), where $2{\cdot}C_{dp}$ is the concentration of the protein-bound monomers in a dimeric form. Furthermore, eqn (4) and (5) were combined under the assumption of different protein binding sites for the dye monomers and dimers. However, *Hypothesis 1a* did not lead to sufficient improvement of the theoretical binding curves. Specifically, for the set of AK7-5/AK7-6 parameters {K_b = 0.02 μM^{-1}, m = 1, K_{bd} = 0.01 μM^{-1}, m_d = 1}/{K_b = 0.03 μM^{-1}, m = 1, K_{bd} = 0.01 μM^{-1}, m_d = 1}, the difference between the calculated A_{640}, A_{700} and A_{840} values was the same or greater than those obtained for *Hypothesis 1*, indicating that AK7-5 and AK7-6 spectral behavior in the presence of native lysozyme is influenced to a minor extent by the dye monomer–protein and dimer–protein binding.

Hypothesis 2. In view of the above rationales, we fail to obtain reasonable values of providing good agreement between the experiment and theory, because the absorbance decrease in the H-band (arising from the breaking of the dye H-aggregates upon the shift of the dye monomer–aggregate equilibrium) is presumably followed by J-aggregate formation of the protein-bound dye monomers. This idea is corroborated by the lower absorptivity values and characteristic bathochromic shifts of lysozyme-bound AK7-5 and AK7-6 with respect to the monomer bands (Fig. 2 and Fig. S4C, D, ESI†),[23,50] and agrees with the previously reported formation of J-aggregates in the presence of BSA.[71] Finally, the estimation of the half-widths of the AK7-5/AK7-6 monomer bands in DMSO at 808/815 nm, and the bands at 840 nm observed in the presence of 35 μM lysozyme, yielded the values $\Delta\nu_{1/2}$ ~ 50/60 nm and ~125/145 nm, respectively, suggesting the appearance of new dye species upon dye complexation with the protein.[13,14] Taking into account the fact that J-aggregates possess narrow absorption bands, the broadband at 840 nm seems to be the superposition of the J-aggregate (of different sizes and molecular packing) and monomer bands. It is also noteworthy that the higher stability of AK7-5 H-aggregates and the lower extent of J-aggregate formation as compared to AK7-6 (Fig. S4C and D, ESI†) could be interpreted in terms of the different polarities of the dye binding sites.[17,27]

Notably, an appropriate theoretical model, allowing quantitative characterization of AK7-5 and AK7-6 complexation with native lysozyme, was not developed because the J-aggregate absorption bands of AK7-5 and AK7-6 are too weak to resolve the quantitative characterization of their formation. Furthermore, inclusion of a new equilibrium between the protein-bound monomers and J-aggregates to the set {(1)–(5)} will significantly complicate the solution of the obtained set of equations.

Cyanine dye response to fibrillar lysozyme

The changes produced by fibrillar lysozyme in the absorption spectra of AK7-5 and AK7-6 were found to differ from those caused by the native protein. As illustrated in Fig. 3A and B, the absorption maxima of H-aggregates are shifted by ~45 nm to longer wavelengths. This effect was accompanied by the absorbance decrease of AK7-5, being less pronounced than that brought about by native lysozyme (~7% at the maximum protein concentration relative to the lowest protein concentration 6.4 μM).

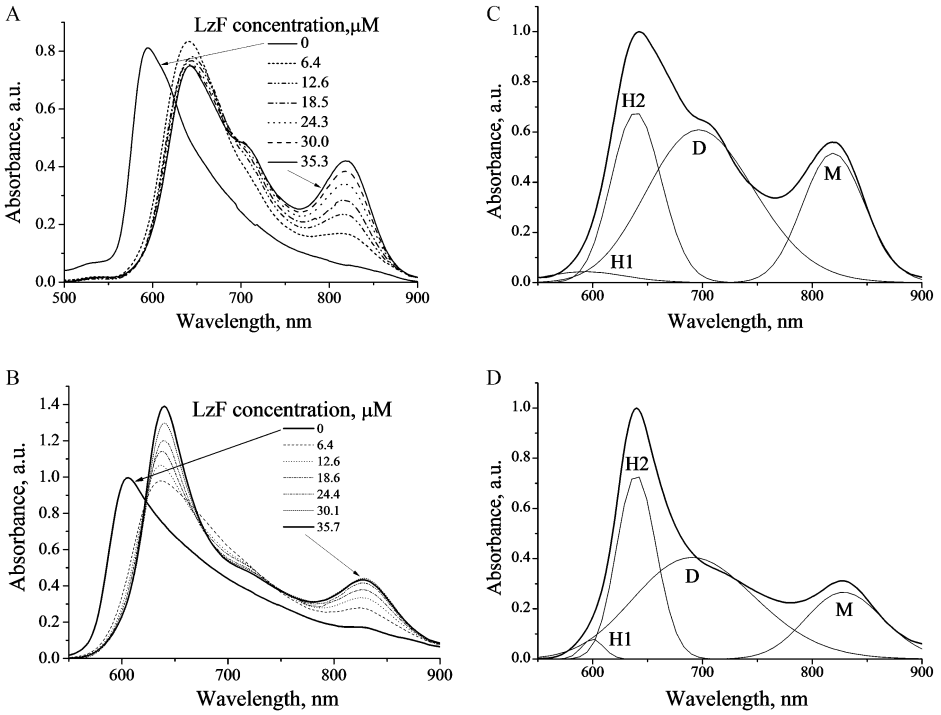

Fig. 3 Absorption spectra of AK7-5 (A) and AK7-6 (B) at an increasing concentration of fibrillar lysozyme (LzN). Normalized absorption spectra of AK7-5 (C) and AK7-6 (D) in the presence of 35.3 μM (C) and 35.7 μM (D) of fibrillar lysozyme. The AK7-5 and AK7-6 concentrations were 12.2 and 13.5 μM, respectively.

Furthermore, the intensity of the AK7-6 H-band was enhanced by a factor of ~1.4 at the maximum protein concentration. At the same time, a shoulder appeared at 700 nm, reflecting the increase of the amount of H-dimer species (Fig. 3A and B). Likewise, the drop in the relative contribution of the H1 band to the overall spectrum was much more pronounced for fibrillar lysozyme, compared to the native protein (Fig. S4C, D, ESI† and Fig. 3C, D). Finally, marked absorbance increases were observed for AK7-5/AK7-6 at 820 nm/830 nm (*ca.* ~7/2.5 times at the maximum protein concentration). The observed red shifts of the dye absorption maxima could result from both the decrease of the environmental polarity[43] and J-aggregate formation. For example, *ca.* 15–27 nm red shift of the monomeric absorption band was observed for pentamethine and thiacarbocyanine dyes bound to bovine serum albumin (BSA) and human serum albumin (HSA), respectively, relative to buffer.[72] Interestingly, the half-widths of the dye absorption bands at 820 nm/830 nm were $\Delta\nu_{1/2} \sim 85$ nm and 90 nm, respectively. Although these values are close to the half-width of the monomer band, the appearance of some amount of J aggregates upon dye incorporation into lysozyme fibrils cannot be excluded. Similarly, the binding of thiacarbocyanine 7514 to insulin amyloid fibrils resulted in the greatly increased absorbance of the band corresponding to the monomeric dye–fibril complex and a slightly enhanced intensity of the dye J-aggregate band.[73] It should be noted in this context that the self-stacked dimers of the cyanine dye YOYO-1 were disrupted in the presence of fibrillar Aβ(1–42) due to the self-stacking to non-stacking transition of the two YO moieties.[74]

Next, the same hypotheses as in the case of native lysozyme have been invoked to explain the spectral behavior of the examined cyanines in the presence of lysozyme fibrils.

Hypothesis 1. First, since the most substantial increases of the AK7-5 absorbance were observed at 820 nm, we found the set of parameters $\{K_b = 0.5\ \mu M^{-1}, m = 0.3, \varepsilon_{820} = 0.197\ \mu M^{-1}\ cm^{-1}\}$ providing good agreement between the experiment and theory, with the difference between the experimental and calculated absorbances being less than 4% at the maximum protein concentration. In contrast, the calculated values of A_{640} ($\varepsilon_{640} = 0.05\ \mu M^{-1}\ cm^{-1}$) and A_{700} ($\varepsilon_{640} = 0.1\ \mu M^{-1}\ cm^{-1}$) were less than the experimental ones by 30.5% and 53%, respectively, at the maximum protein concentration. Similarly, for AK7-6 the following parameter set $\{K_b = 0.5\ \mu M^{-1}, m = 0.3, \varepsilon_{830} = 0.197\ \mu M^{-1}\ cm^{-1}\}$ provided a difference between the experimental and calculated absorbances at 830 nm of less than 16% at the maximum protein concentration. The values of A_{640} ($\varepsilon_{640} = 0.1\ \mu M^{-1}\ cm^{-1}$) and A_{700} ($\varepsilon_{640} = 0.197\ \mu M^{-1}\ cm^{-1}$) were less than the experimental ones by 17% and 35%, respectively. Thus, the assumption that only the dye monomers are capable of associating with lysozyme fibrils cannot reproduce the behavior of the H-dimers and H-aggregates with sufficient accuracy.

Hypothesis 1a. It cannot be excluded that the binding of both the dye monomers and H-dimers to fibrillar lysozyme accounts for the observed spectral effects. By numerically solving eqn (3)–(5), we found a set of parameters $\{K_b = 0.6\ \mu M^{-1}, m = 0.3, K_{bd} = 0.2\ \mu M^{-1}, m_d = 0.8\}$ for AK7-5, providing good agreement between the experimental and calculated values of A_{820}, A_{700}

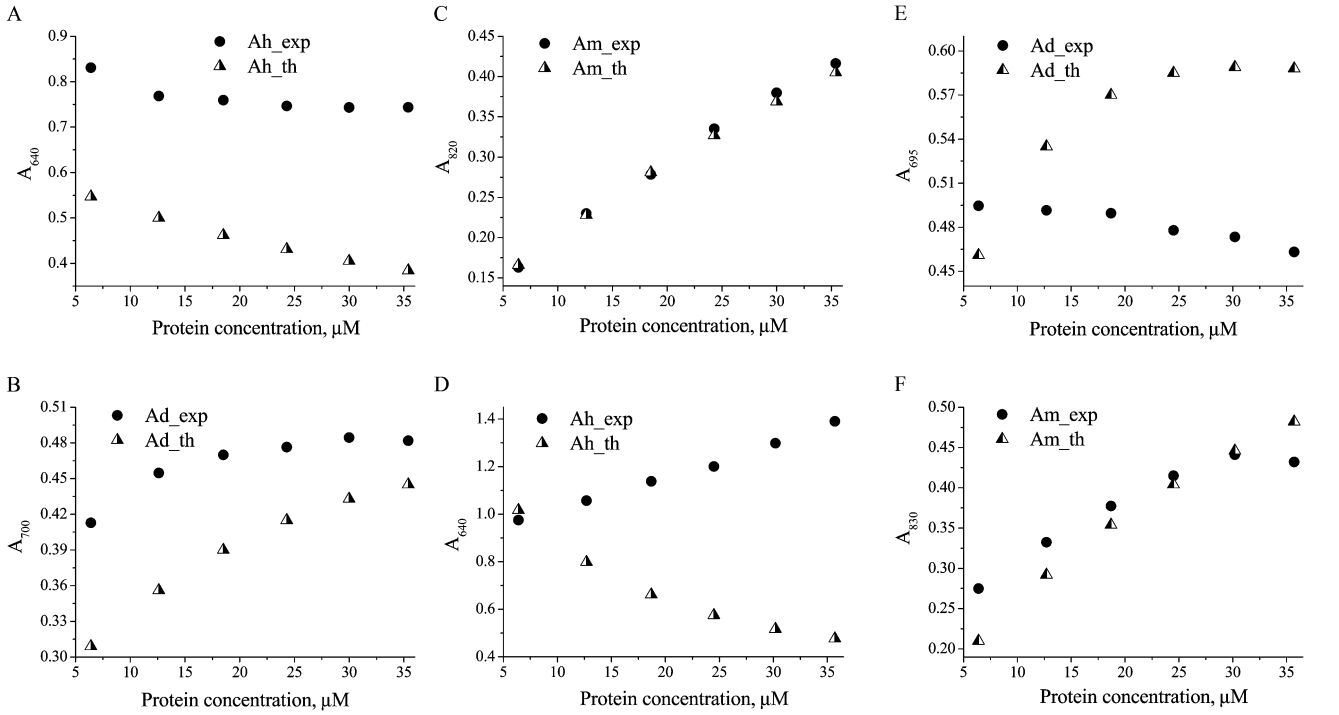

Fig. 4 The measured (Am_exp) and theoretically predicted (Am_th) absorbances of the AK7-5/AK7-6 H-aggregates (A and D), H-dimers (B and E) and monomers (C and F) in the presence of fibrillar lysozyme, calculated using the following sets of parameters: {K_b = 0.6 μM^{-1}, m = 0.3, K_{bd} = 0.2 μM^{-1}, m_d = 0.8, K_h = 85, K_d = 7 μM^{-1}, n = 4}/{K_b = 0.8 μM^{-1}, m = 0.35, K_{bd} = 0.3 μM^{-1}, m_d = 2, K_h = 120, K_d = 5 μM^{-1}, n = 4}.

and A_{640} (the difference between the absorbances was less that 3%, 8% and 48%, respectively, at the maximum protein concentration). Fig. 4A–C represents the measured and calculated absorbances at 640, 700 and 820 nm over the overall protein concentration range. This suggests that the behavior of AK7-5 in the lysozyme fibril system could be adequately described in terms of dye monomer–protein and dimer–protein binding. In contrast, for the set of parameters {K_b = 0.8 μM^{-1}, m = 0.35, K_{bd} = 0.3 μM^{-1}, m_d = 2} recovered in an analogous way for AK7-6, the difference between the experimental and calculated values of A_{830}, A_{700} and A_{640} was ~9%, 21% and 66%, respectively, at the maximum protein concentration. Fig. 4D–F represents the measured and calculated absorbances at 640, 700 and 830 nm over the overall lysozyme concentration range. Notably, as shown in Fig. 4D, theory predicts the linear drop in the AK7-6 H-aggregate concentration, the effect being opposite to that observed in the experiment.

Hypothesis 2. It seems likely that the observed minor discrepancies between the measured and calculated absorbances of AK7-5 H-aggregates and AK7-6 dimers result from the formation of J-aggregates by the part of the dye monomer species incorporated into the fibrils. The protein-bound H-dimer species of AK7-6 could also transform into J-aggregates, because AK7-6 H-dimer absorption is decreased upon increasing the protein concentration (Fig. 4E).

Hypothesis 2a. Furthermore, a significant difference between the measured and predicted intensities of the AK7-6 H-band could result from the formation of H-aggregates with a lower aggregation number compared to those observed in buffer. This could be, for instance, AK7-6 trimers. Thus, it appeared that, in contrast to AK7-5, the AK7-6 monomer binding to lysozyme fibrils is followed by the formation of trimer species by some of the protein-bound dye. This process is very complex and can be explained only qualitatively. Our results are in accordance with those obtained for the negatively charged pinacyanol dye associated with fibrillar Aβ,[26] for the cyanine dye bound to the DNA groove,[75] and for Thiazole Orange adsorbed on a calix[4]arene sulfonate template.[76] Specifically, the formation of H-aggregates was observed at increasing fibril or DNA concentration, although no aggregation occurred upon the dye binding to random coil and α-conformations.

Summarizing the above results, we concluded that *Hypotheses 1a*, *2* and *2a* can adequately reproduce the behavior of AK7-5 and AK7-6, respectively, in the presence of lysozyme fibrils.

Photophysical properties of cyanine dyes and their affinity for lysozyme

As provided in Table S1 (ESI†), AK7-5 and AK7-6 display high lipophilicity ($C\log P$) values, which are comparable with the affinity of cyanines for the hydrophobic cavities of BSA.[71,77] Notably, a greater constant of AK7-6 binding to native lysozyme can account for its larger $C\log P$ value (Table S1, ESI†), suggesting a less polar environment of the dye in the protein-bound state.[74]

Interestingly, the constants for the AK7-5/AK7-6 monomer binding to lysozyme fibrils were ~1 order of magnitude greater than those for the native protein and ~3 times higher than those for the AK7-5/AK7-6 H-dimer complexation with fibrils.

Such high affinities and stoichiometries are similar to those of Thioflavin T,[69] which could be explained by the presence of amino substituents in the dye heterocycles as was revealed for mono- and trimethine cyanine dyes.[78] Furthermore, QSAR studies predicted that lipophilicity, the size of the aromatic system, solvent accessible surface area, dipole moment, *etc.*, determine the dye affinity for amyloid fibrils.[79] Indeed, AK7-5 and AK7-6 have ~50% greater CA values than those found for another class of potential amyloid markers, benzanthrone dyes, and greater affinities for lysozyme fibrils than the majority of benzanthrones.[80] AK7-5 and AK7-6 also have ~2 times lower μ_g values and HOMO–LUMO energy gaps as compared to benzanthrones (Table S1, ESI†), pointing to weaker solvatochromism and lower kinetic stability of the NIR dyes.[81]

Potential lysozyme binding sites for the novel cyanine dyes

Simple docking studies showed that the novel dyes interact with the deep cleft of native lysozyme lined with both hydrophobic and negatively charged residues.[82] It appeared that the cleft volume is sufficient to accommodate the monomer and dimer dye species (Fig. 5). The hydrophobic dye–protein interactions are likely to be predominant, similar to the case of cyanine binding to HSA. Furthermore, in view of the fact that cyanine J-aggregates are formed on the negatively charged DNA templates,[82] it can be assumed that electrostatic interactions between the positively charged dyes under study and negatively charged amino acids E53, E35, D52 and D70 of the lysozyme active site significantly stabilize the structure of J-aggregates of AK7-5 and AK7-6.

Due to their high affinities for lysozyme fibrils, the monomers of AK7-5 and AK7-6 are most likely incorporated into the fibril grooves representing specific binding sites for the amyloid markers.[83] Likewise, the binding to fibril grooves has been observed for monomethinecyanines, trimethinecyanines and the cyanine dye YOYO-1.[27,76] Notably, the calculated lengths, widths and heights of the optimized AK7-5 and AK7-6 structures were ~2.1, 1.3 and 0.6 nm (Table S1, ESI†), while the distance between the every second residue and the interstrand distance in the β-sheet are ~0.7 nm and ~0.4 nm, respectively.[84] Therefore, the dye monomer species should associate with 5 β-strands in such a way that their short axis is perpendicular to the fibril axis. Our suggestions are also confirmed by the docking studies, which revealed the most energetically favourable AK7-5/AK7-6 binding in the Q75–N59/S60–W62, G54–L56 grooves of the lysozyme fibril core (Fig. 6). Notably, aromatic substituents in the AK7-6 molecule, possessing higher affinity for lysozyme fibrils than AK7-5, interact with tryptophan residues of the S60_W62/L54_G56 channel, forming the most energetically favourable complex with the dye (Fig. 6). Similarly, classical amyloid marker Thioflavin T preferentially interacted with the grooves, containing aromatic residues, as revealed from *in silico* studies.[85]

In turn, according to our docking results, the AK7-5 and AK7-6 dimer species seem to occupy the non-specific protein

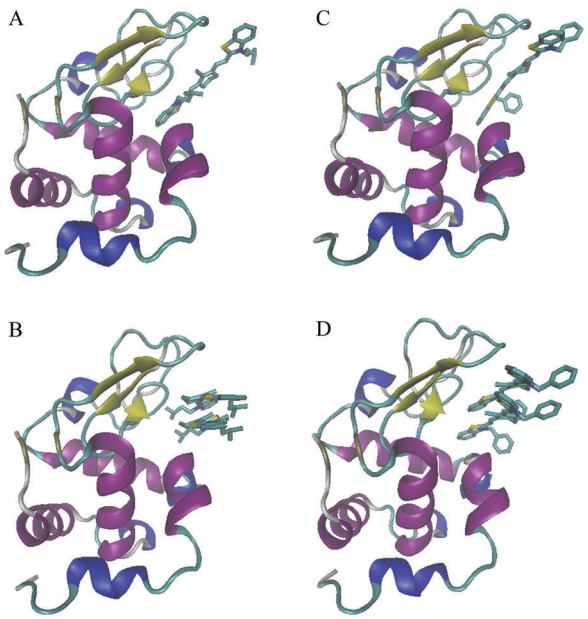

Fig. 5 Schematic representation of the AK7-5/AK7-6 monomer (A and C) and dimer (B and D) complexes with native lysozyme, obtained using PatchDock/FireDock servers. The dyes are bound to a deep protein cleft, which comprises the lysozyme active site. The protein molecule is colored according to its secondary structure: helices (magenta and blue), beta-sheet (yellow), turns (cyan) and coil (white).

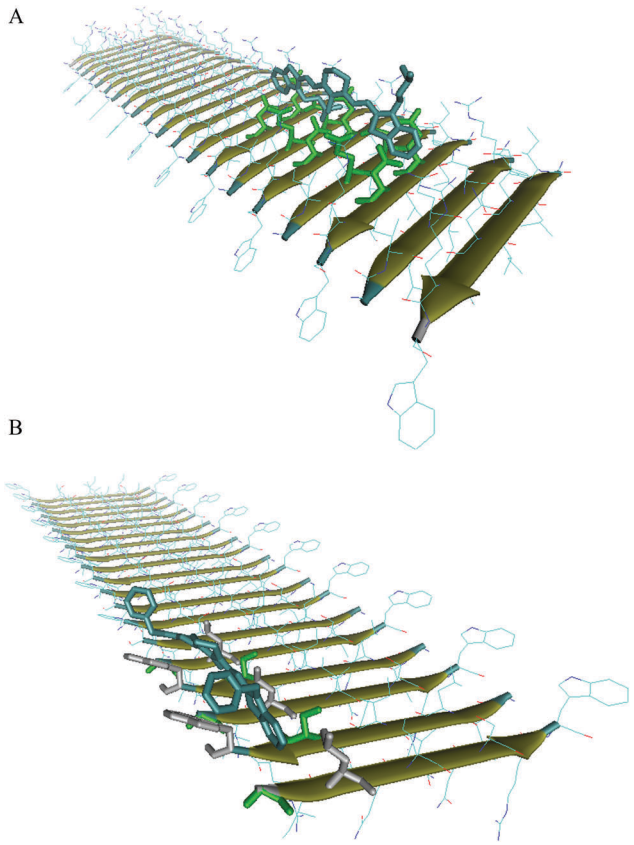

Fig. 6 Schematic representation of the AK7-5 (A) and AK7-6 (B) complexes with the lysozyme fibril core (represented by the β-sheet formed from the K-peptide), obtained using PatchDock/FireDock servers. AK7-5 is bound to the Q57_N59/N59_Q57 fibril groove, and AK7-6 is associated with the S60_W62/L54_G56 fibril groove of the anti-parallel β-sheet. Polar and nonpolar residues are colored in green and grey, respectively.

sites, lying perpendicular to the fibril axis. Similarly, the high affinity of Thiazole Orange monomers for DNA was explained by the dye stacking with DNA bases, while dimers possessing low affinity (due to steric restrictions) were assumed to interact with the external surface of the DNA molecule in a way that prevents stacking of one monomer subunit with the DNA bases.[86] Notably, the above estimate of the size of AK7-6 H-aggregates formed on the fibril surface ($n \approx 3$) was about one order of magnitude lower than that of cyanine aggregates obtained in liposomal and DNA systems, presumably due to steric restrictions for the dimer binding to fibril grooves.[87]

According to the docking studies, unlike native lysozyme, fibril binding sites for the examined dyes are represented by grooves formed by polar and nonpolar amino acid residues (Fig. 6). This can explain the less pronounced formation of J-aggregates in the presence of fibrillar lysozyme compared to the native protein.[87] Notably, electrostatic attraction and hydrophobic interactions play a significant role in cyanine dye L-21 aggregate formation on the DNA template.[88] H-aggregate dissociation into monomers and subsequent J-aggregate formation are presumably controlled by the strong monomer–protein hydrophobic and dye–dye electrostatic interactions.[89] Obviously, partial ejection of the bulky AK7-6 dye from the fibril groove (Fig. 6) shifts the equilibrium towards the formation of H-aggregates on the fibril surface. Indeed, the AK7-6 binding groove resides on the nonpolar surface of the lysozyme β-sheet.[58] Therefore, lateral association of the two β-sheets results in the formation of the dry ''steric zipper'' interface that is sterically less accessible for the dyes than the polar face of the fibril (Fig. 6).[83]

Interestingly, the spectral behavior of AK7-5 and AK7-6 in the presence of fibrillar lysozyme was similar to that observed upon their binding to BSA, being indicative of the predominant role of the dye monomer–protein hydrophobic and dye–dye electrostatic interactions in the disruption of H-aggregates incorporated into the amyloid species as well.[51] Furthermore, the examined dyes displayed high lipophilicity.[89] In view of the above rationales, we concluded that fibril grooves are not unique high-affinity binding sites for AK7-5 and AK7-6, although analysis of the absorption spectra allows highly sensitive *in vitro* differentiation between native and fibrillar lysozyme. Taken together, these results indicate that AK7-5 and AK7-6 can be employed for amyloid fibril detection using absorption spectroscopy.

Conclusions

In conclusion, the present study was focused on the quantitative characterization of the binding of heptamethine cyanine dyes AK7-5 and AK7-6 to native and fibrillar lysozyme, taking into account the ability of the dyes to self-associate in buffer. An adequate model for the cyanine aggregation behavior was proposed, assuming dye monomer and dimer association with the protein, in addition to dye aggregation in buffer. The obtained results showed that AK7-5 and AK7-6 display high affinity for lysozyme fibrils and different aggregation extents in the presence of monomeric and fibrillar proteins, rendering these probes suitable for the noncovalent labeling of amyloid fibrils. The dye–fibril hydrophobic interactions and steric hindrances are supposed to have the predominant influence on the association of AK7-5 and AK7-6 with fibrillar lysozyme.

Acknowledgements

This work was supported by the Ministry of Education and Science of Ukraine (the Young Scientist project ''Design of the novel methods of fluorescence diagnostics of amyloid pathologies'').

References

1 J. Fabian, H. Nakazumi and M. Matsuoka, *Chem. Rev.*, 1992, **92**, 1197–1226.
2 H. Berlepsch, E. Brandenburg, B. Koksch and C. Böttcher, *Langmuir*, 2010, **26**, 11452–11460.
3 M. Guo, P. Diao, Y.-J. Ren, F. Meng, H. Tian and S.-M. Cai, *Sol. Energy Mater. Sol. Cells*, 2005, **88**, 33–35.
4 F. Welder, B. Paul, H. Nakazumi, S. Yagi and C. L. Colyer, *J. Chromatogr. B: Anal. Technol. Biomed. Life Sci.*, 2003, **793**, 93–105.
5 S. M. Yarmoluk, V. B. Kovalska and K. D. Volkova, *Adv. Fluor. Report. Chem. Biol. III*, 2011, **113**, 161–199.
6 A. Mishra, R. K. Behera, P. K. Behera, B. K. Mishra and G. B. Behera, *Chem. Rev.*, 2000, **100**, 1973–2011.
7 Z. Lou, P. Li and K. Han, *Acc. Chem. Res.*, 2015, **48**, 1358–1368.
8 F. Yu, P. Li, G. Li, G. Zhao, T. Chu and K. Han, *J. Am. Chem. Soc.*, 2011, **133**, 11030–11033.
9 N. I. Gadjev, T. G. Deligeorgiev and S. H. Kim, *Dyes Pigm.*, 1999, **40**, 181–186.
10 A. S. Waggoner, C. H. Wang and R. L. Tolles, *J. Membr. Biol.*, 1977, **33**, 109–140.
11 G. Patonay, J. S. Kim, R. Kodagahally and L. Strekowski, *Appl. Spectrosc.*, 2005, **59**, 682–690.
12 M. K. Johansson, H. Fidder, D. Dick and R. M. Cook, *J. Am. Chem. Soc.*, 2002, **124**, 6950–6956.
13 R. F. Khairutdinov and N. Serpone, *J. Phys. Chem. B*, 1997, **101**, 2602–2610.
14 A. Eisfeld and K. J. S. Briggs, *Chem. Phys.*, 2006, **324**, 376–384.
15 M. Kasha, H. R. Rawls and M. Ashraf El-Bayoumi, *Pure Appl. Chem.*, 1965, **11**, 371–392.
16 J. S. Kim, R. Kodagahally, L. Strekowski and G. Patonay, *Talanta*, 2005, **67**, 947–954.
17 A. A. Ishchenko, *Russ. Chem. Rev.*, 1991, **60**, 865–884.
18 J. Kang, O. Kaczmarek, J. Liebscher and L. Dähne, *Int. J. Polym. Sci.*, 2010, **264781**, 1–7.
19 V. B. Kovalska, M. Yu. Losytskyy, S. V. Chernii, V. Ya. Chernii, I. M. Tretyakova, S. M Yarmoluk and S. V. Volkov, *Biopolym. Cell*, 2013, **29**, 473–479.
20 R. F. Pasternack, C. Fleming, S. Herring, P. J. Collings, J. dePaula, G. DeCastro and E. J. Gibbs, *Biophys. J.*, 2000, **79**, 550–560.
21 Y. Zhang, J. Xiang, Y. Tang, G. Xu and W. Yan, *Dyes Pigm.*, 2008, **76**, 88–93.

22 S. Gadde, E. K. Batchelor and A. E. Kaifer, *Chemistry*, 2009, **15**, 6025–6031.
23 A. S. Tatikolov and S. M. B. Costa, *Chem. Phys. Lett.*, 2001, **346**, 233–240.
24 V. N. Uversky and A. L. Fink, *Biochim. Biophys. Acta*, 2004, **1698**, 131–153.
25 B. H. Toyama and J. S. Weissman, *Annu. Rev. Biochem.*, 2011, **80**, 557–585.
26 R. Sabate and J. Estelrich, *Biopolymers*, 2003, **72**, 455–463.
27 K. D. Volkova, V. B. Kovalska, A. O. Balanda, M. Y. Losytskyy, A. G. Golub, R. J. Vermeij, V. Subramaniam, O. I. Tolmachev and S. M. Yarmoluk, *Bioorg. Med. Chem.*, 2008, **16**, 1452–1459.
28 K. Chegaev, A. Federico, E. Marini, B. Rolando, R. Fruttero, M. Morbin, G. Rossi, V. Fugnanesi, A. Bastone, M. Salmona, N. B. Badiola, L. Gasparini, S. Cocco, C. Ripoli, C. Grassi and A. Gasco, *Bioorg. Med. Chem.*, 2015, **23**, 4688–4698.
29 K. D. Volkova, V. B. Kovalska, D. Inshin, Y. L. Slominskii, O. I. Tolmachev and S. M. Yarmoluk, *Biotech. Histochem.*, 2011, **86**, 188–191.
30 W. Yang, Y. Wong, O. T. W. Ng, B. L.-P. Bai, D. W. J. Kwong, Y. Ke, Z.-H. Jiang, H.-W. Li, K. L. K. Yung and M. S. Wong, *Angew. Chem., Int. Ed.*, 2012, **51**, 1804–1810.
31 J. Kuret, C. N. Chirita, E. E. Congdon, T. Kannanayakal, G. Li, M. Necula, H. Yin and Q. Zhohg, *Biochim. Biophys. Acta*, 2005, **1739**, 167–178.
32 V. Kovalska, M. Losytskyy, V. Chernii, K. Volkova, I. Tretyakova, V. Cherepanov, S. Yarmoluk and S. Volkov, *Bioorg. Med. Chem.*, 2012, **20**, 330–334.
33 V. B. Kovalska, M. Y. Losytskyy, O. I. Tolmachev, Y. L. Slominskii, G. M. Segers-Nolten, V. Subramaniam and S. M. Yarmoluk, *J. Fluoresc.*, 2012, **22**, 1441–1448.
34 C. D. Geddes, H. Cao and J. R. Lakowicz, *Spectrochim. Acta, Part A*, 2003, **59**, 2611–2617.
35 A. Sanchez-Galvez, P. Hunt, M. A. Robb, M. Olivucci, T. Vreven and H. B. Schlegel, *J. Am. Chem. Soc.*, 2000, **122**, 2911–2924.
36 J. Pauli, T. Vag, R. Haag, M. Spieles, M. Wenzel, W. A. Kaiser, U. Resch-Genger and I. Hilger, *Eur. J. Med. Chem.*, 2009, **44**, 3496–3503.
37 Z. Zhang and S. Achilefu, *Org. Lett.*, 2004, **6**, 2067–2070.
38 A. M. Kragh, R. Peacock and G. S. Reddy, *J. Photogr. Sci.*, 1966, **14**, 185–198.
39 E. Chang, E. E. Congdon, N. S. Honson, K. E. Duff and J. Kuret, *J. Med. Chem.*, 2009, **52**, 3539–3547.
40 S. A. Soper and Q. L. Mattingly, *J. Am. Chem. Soc.*, 1994, **116**, 3744–3752.
41 E. D. Moody, P. J. Viskari and C. L. Colyer, *J. Chromatogr. B: Biomed. Sci. Appl.*, 1999, **729**, 55–64.
42 S. McConnell, R. H. McKenzie and S. Olsen, *J. Chem. Phys.*, 2015, **142**, 084502.
43 J. L. Seifert, R. E. Connor, S. A. Kushon, M. Wang and B. A. Armitage, *J. Am. Chem. Soc.*, 1999, **121**, 2987–2995.
44 M. Y. Berezin, H. Lee, W. Akers, K. Guo, R. J. Goiffon, A. Almutairi, J. M. Fréchet and S. Achilefu, *Conf. Proc. IEEE Eng. Med. Biol. Soc.*, 2009, **2009**, 114–117.
45 S. Upadhyayula, V. Nuñez, E. M. Espinoza, J. M. Larsen, D. Bao, D. Shi, J. T. Mac, B. Anvaria and V. I. Vullev, *Chem. Sci.*, 2015, **6**, 2237–2251.
46 G.-J. Zhao, J.-Y. Liu, L.-C. Zhou and K.-L. Han, *J. Phys. Chem. B*, 2007, **111**, 8940–8945.
47 G.-J. Zhao and K.-L. Han, *Biophys. J.*, 2008, **94**, 38–46.
48 G.-J. Zhao and K.-L. Han, *Acc. Chem. Res.*, 2012, **45**, 404–413.
49 L. Strekowski, M. Lipowska and G. Patonay, *J. Org. Chem.*, 1992, **57**, 4578–4580.
50 K. Kemnitz, K. Yoshihara and T. Tani, *J. Phys. Chem.*, 1990, **94**, 3099–3104.
51 A. Kurutos, O. Ryzhova, U. Tarabara, V. Trusova, G. Gorbenko, N. Gadjev and T. Deligeorgiev, *J. Photochem. Photobiol., A*, 2016, **328**, 87–96.
52 N. Nizomov, E. N. Kurtaliev, S. N. Nizamov and G. Khodjayev, *J. Mol. Struct.*, 2009, **936**, 199–205.
53 L. A. Morozova-Roche, J. Zurdo, A. Spencer, W. Noppe, V. Receveur, D. B. Archer, M. Joniau and C. M. Dobson, *J. Struct. Biol.*, 2000, **130**, 339–351.
54 M. W. Schmidt, K. K. Baldridge, J. A. Boatz, S. T. Elbert, M. S. Gordon, J. H. Jensen, S. Koseki, N. Matsunaga, K. A. Nguyen, S. J. Su, T. L. Windus, M. Dupuis and J. A. Montgomery, *J. Comput. Chem.*, 1993, **14**, 1347–1363.
55 J. S. Binkley, J. A. Pople and W. J. Hehre, *J. Am. Chem. Soc.*, 1980, **102**, 939–947.
56 E. Runge and E. K. U. Gross, *Phys. Rev. Lett.*, 1984, **52**, 997–1000.
57 V. Trusova, *East European Journal of Physics*, 2015, **2**, 51–58.
58 M. Smaoui, *Biophys. J.*, 2013, **104**, 683–693.
59 D. Duhovny, R. Nussinov and H. J. Wolfson, *Lect. Notes Comput. Sci. Eng.*, 2002, **2452**, 185–200.
60 E. Mashiach, D. Schneidman-Duhovny, N. Andrusier, R. Nussinov and H. J. Wolfson, *Nucleic Acids Res.*, 2008, **36**, 229–232.
61 L. F. Vieira Ferreira, A. S. Oliveira, F. Wilkinsonb and D. Worrallb, *J. Chem. Soc., Faraday Trans.*, 1996, **92**, 1217–1225.
62 O. K. Kim, J. Je, G. Jernigan, L. Buckley and D. Whitten, *J. Am. Chem. Soc.*, 2006, **128**, 510–516.
63 M. Wang, G. L. Silva and B. A. Armitage, *J. Am. Chem. Soc.*, 2000, **122**, 9977–9986.
64 R. A. Garoff, E. A. Litzinger, R. E. Connor, I. Fishman and B. A. Armitage, *Langmuir*, 2002, **18**, 6330–6337.
65 S. Tai and N. Hayashi, *J. Chem. Soc., Perkin Trans. 2*, 1991, 1275–1279.
66 W. Huang, L.-Y. Wang, Y.-L. Fu, J.-Q. Liu, Y.-N. Tao, F.-L. Fan, G.-H. Zhai and Z.-Y. Wen, *Bull. Korean Chem. Soc.*, 2009, **30**, 556–560.
67 W. J. Schutte, M. Sluyters-Rehbach and J. H. Sluyters, *J. Phys. Chem.*, 1993, **97**, 6069–6073.
68 U. Rösch, S. Yao, R. Wortmann and F. Würthner, *Angew. Chem., Int. Ed.*, 2006, **45**, 7026–7030.
69 A. I. Sulatskaya, I. M. Kuznetsova and K. K. Turoverov, *J. Phys. Chem. B*, 2011, **115**, 11519–11524.
70 W. E. Klunk, J. W. Pettegrew and D. J. Abraham, *J. Histochem. Cytochem.*, 1989, **37**, 1273–1281.

71 D. S. Pisoni, L. Todeschini, A. C. A. Borges, C. L. Petzhold, F. S. Rodembusch and L. F. Campo, *J. Org. Chem.*, 2014, **79**, 5511–5520.
72 Y.-Z. Zhang, Q.-F. Yang, H.-Y. Du, Y.-L. Tang, G.-Z. Xu and W.-P. Yan, *Chin. J. Chem.*, 2008, **26**, 397–401.
73 K. D. Volkova, V. B. Kovalska, M. Y. Losytskyy, K. O. Fal, N. O. Derevyanko, Y. L. Slominskii, O. I. Tolmachov and S. M. Yarmoluk, *J. Fluoresc.*, 2011, **21**, 775–784.
74 D. J. Lindberg and E. K. Esbjörner, *Biochem. Biophys. Res. Commun.*, 2016, **469**, 313–318.
75 K. C. Hannah and B. A. Armitage, *Acc. Chem. Res.*, 2004, **37**, 845–853.
76 V. Lau and B. Heyne, *Chem. Commun.*, 2010, **46**, 3595–3597.
77 Y. V. Malyukin, I. A. Borovoi, N. S. Kavok, A. V. Gerashchenko, N. L. Pogrebnyak, S. L. Efimova and A. N. Lebedenko, *Biophysics*, 2007, **52**, 406–411.
78 K. D. Volkova, V. B. Kovalska, A. O. Balanda, Y. L. Slominskii, O. I. Tolmachev, V. Subramaniam and S. M. Yarmoluk, *Ukrainian Bioorganic Acta*, 2008, **6**, 15–21.
79 K. Cisek and J. Kuret, *Bioorg. Med. Chem.*, 2012, **20**, 1434–1441.
80 O. Ryzhova, K. Vus, V. Trusova, E. Kirilova, G. Kirilov, G. Gorbenko and P. Kinnunen, *Methods Appl. Fluoresc.*, 2016, **4**, 034007.
81 M. Y. Berezin, H. Lee, W. Akers and S. Achilefu, *Biophys. J.*, 2007, **93**, 2892–2899.
82 N. M. Godjayev, S. Akyüz and L. Ismailova, *Int. J. Phys. Eng. Sci.*, 1998, **51**, 56–60.
83 K. Vus, V. Trusova, G. Gorbenko, R. Sood, E. Kirilova, G. Kirilov, I. Kalnina and P. Kinnunen, *J. Fluoresc.*, 2014, **24**, 493–504.
84 M. R. Krebs, E. H. Bromley and A. M. Donald, *J. Struct. Biol.*, 2005, **149**, 30–37.
85 M. Biancalana and S. Koide, *Biochim. Biophys. Acta*, 2010, **1804**, 1405–1412.
86 M. V. Kuperman, S. V. Chernii, M. Yu. Losytskyy, D. V. Kryvorotenko, N. O. Derevyanko, Y. L. Slominskii, V. B. Kovalska and S. M. Yarmoluk, *Anal. Biochem.*, 2015, **484**, 9–17.
87 T. Y. Ogulchansky, M. Y. Losytskyy, V. B. Kovalska, S. S. Lukashov, V. M. Yashchuk and S. M. Yarmoluk, *Spectrochim. Acta, Part A*, 2001, **57**, 2705–2715.
88 G. Y. Guralchuk, A. V. Sorokin, I. K. Katrunov, S. L. Yefimova, A. N. Lebedenko, Y. V. Malyukin and S. M. Yarmoluk, *J. Fluoresc.*, 2007, **17**, 370–376.
89 A. Kurutos, O. Ryzhova, V. Trusova, U. Tarabara, G. Gorbenko, N. Gadjev and T. Deligeorgiev, *Dyes Pigm.*, 2016, **130**, 122–128.